Proceedings of 15th IOE Graduate Conference
Peer Reviewed
Year: 2024 Month: May Volume: 15
ISSN: 2350-8914 (Online), 2350-8906 (Print)

Landslide Susceptibility Mapping Under Climate Change Scenarios Using XGBoost Algorithm

Arhat Ratna Kansakar [a], Bhim Kumar Dahal [b]

[a] *Department of Applied Science and Chemical Engineering, Pulchowk Campus, IOE, Tribhuvan University, Nepal*
[b] *Department of Civil Engineering, Pulchowk Campus, IOE, Tribhuvan University, Nepal*
[a] 78msccd003.arhat@pcampus.edu.np, [b] bhimd@pcampus.edu.np

Abstract
Rainfall can be considered an important landslide-triggering factor in Nepal as most landslides occur during the monsoon season. Climate change is projected to amplify the frequency and intensity of precipitation events. Extreme hydro-meteorological conditions induced by climate change can increase the occurrence of landslides in geologically fragile regions like Nepal. We investigated the susceptibility of landslide events under different future Shared Socio-economic Pathways (SSPs) scenarios in Lamjung district. Landslide susceptibility maps were developed for the baseline period (1995-2020), and future climate scenarios were prepared with a set of three Coupled Model Inter-comparison Project (CMIP6) models under SSP245 and SSP585 for the near future (2021-2045), mid-future (2046-2070) and far future (2071- 2095). A machine learning algorithm XGBoost was utilized to generate landslide susceptibility maps. Twelve multivariate factors contributing to landslides were considered including terrain slope, aspect, elevation, curvature, TWI, SPI, geology, soil, distance from the stream, distance from the road, land use/ land cover, and mean annual rainfall, with rainfall selected as a dynamic factor. Further, metrics like Accuracy, Recall, Precision, F1-Score, and Area under the Curve (AUC) were used to assess the model quality. Seven landslide susceptibility maps were developed, classified into five susceptible classes, and compared. The baseline susceptibility maps show that 2.88% and 3.29% of the study area lie in high and very high susceptibility classes. Among the eight municipalities within the study region, Dordi and Marsyangdi rural municipalities exhibit the highest susceptibility to landslides in the baseline period. However, in future landslide susceptibility scenarios, Dudhpokhari, Kwaholasothar, Madhyanepal, and Sundarbazar municipalities are projected to experience a significant increase in landslide areas. The future landslide susceptibility results show an increase in the high and very high susceptibility classes for both SSP245 and SSP585 scenarios compared to the baseline landslide susceptibility map.

Keywords
Landslide susceptibility, CMIP6, XGBoost, Climate change, Precipitation projection

1. Introduction

Landslides are geological events defined as the gravitational movement of earth elements, such as rock, debris, and soil, downslope. Its inherently weak geology, intense and improper land use practices, and seasonal monsoon rains, combined with the tectonically active nature of the Himalayan mountain chain make Nepal susceptible to natural hazards like landslides, debris flows, and soil erosion [1].

The likelihood of landslides occurring in a given location is known as landslide susceptibility and is determined by several conditioning factors that contribute to slope failure [2]. Landslide Susceptibility Mapping (LSM) is a process that involves evaluating an area's susceptibility to landslides by examining and analyzing the elements that contribute to the slope instability. This mapping technique integrates diverse data sources like topography, geology, soil properties, land cover, rainfall patterns, and historical landslide occurrences into a Geographic Information System (GIS) framework to spatially analyze factors, generating susceptibility maps that depict varying levels of landslide vulnerability across different areas.

There are several approaches for developing landslide susceptibility like direct mapping [3], deterministic approach [4], heuristic model [5], probabilistic model [6], and machine learning models [7, 8]. Production of susceptibility maps has become less challenging with advances in processing power, geographic techniques, and machine learning (ML) algorithms.

With the advancement in machine learning, various algorithms have been utilized for landslide susceptibility mapping such as Logistic Regression (LR), Random Forest (RF), Support Vector Machine (SVM) et cetera. In this study, we use the XGBoost algorithm for the landslide susceptibility mapping. In comparison to other machine learning algorithms, Merghadi et al. [9] found that tree-based ensemble algorithms outperformed other machine learning approaches in terms of performance and suitability. Similarly, Pyakurel et al. [8] evaluated LR, RF, SVM, XGBoost, and Extremely Randomized Trees Classifier (ET) algorithms for predicting earthquake-induced landslide susceptibility, noting that XGBoost performed better than LR, RF, and SVM algorithms, with slightly lower performance compared to ET.

1.1 Effect of Climate Change on Landslides

Global climate change is one of the biggest problems facing the modern world. The Earth system and societies are already facing challenges due to threats associated with climate change. Nepal is currently grappling with the consequences of climate change, which include rising temperatures, shifts in

precipitation patterns, and the gradual disappearance of glaciers. A study of the monsoon rainfall period from 1971 to 2005 shows that there is a linear increasing trend of about 2.08 mm/year with large inter-annual variation [10]. The IPCC special report has expressed high confidence in the notion that the escalating alteration in heavy precipitation will influence the occurrence of landslides in certain global regions [11].

Research undertaken in Taiwan [12], China [13], Greece [14], and Italy [15] have shown that climate change will result in an increase in the frequency of shallow, rapid landslides as well as an expansion to their extent. Studies conducted by Wijaya et al. [16], and Nefros et al. [14] have shown that climate change affects slope stability. The results showed that the area of high and very high susceptibility zones will increase in the future, in line with the climate change effect where rainfall and temperature are projected to increase. Research conducted in Nepal over the past few decades has shown rising trends in landslides [17] and extreme precipitation [18]. A study by K.C. et al. [19] on the spatial and temporal analysis of landslides shows a significant correlation between landslides with monthly rainfall, with an intensive cluster of 93.26 % of total landslides during the rainy season.

This study aims to map landslide susceptibility in Lamjung district using the XGBoost algorithm for a baseline (1995-2020) scenario and three future time horizons: near future (2021-2045), mid-future (2046-2070), and far future (2071-2095) under SSP245 and SSP585 climate scenario.

2. Materials and Methodology

2.1 Study Area

Lamjung district is situated in the mid-hill regions of Nepal, with its geography extending to the foothills of the Himalayas. It is located in between latitudes of 28°03'10"and 28°30'36" N, and longitudes of 84°11'22"- 84°41'51" E, with elevation ranging from 373 m to 7870 m.

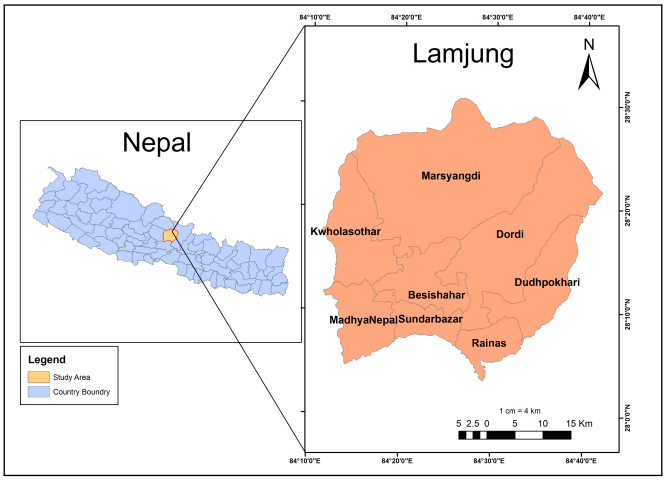

Figure 1: Location of study area

It shares its eastern and western borders with Gorkha and Kaski while it is bordered by Manang and Tanahun districts in the north and the south respectively. Lamjung district covers an area of 1692 km^2. On average, the annual temperature ranges from a minimum of 14.1°C to a maximum of 26.7°C, while the annual precipitation is recorded as 2944.23mm.

2.2 Landslide Triggering Maps

In landslide susceptibility mapping, landslide triggering factor maps play a critical role in assessing and understanding the factors that contribute to landslide occurrence. These maps depict various geological, geo-morphological, climatic, and anthropogenic factors that can trigger landslides. The factors considered in this study are presented in Table 1 along with their sources.

Table 1: Landslide triggering factors and data source

S.N	Factors	Source
1.	Slope Angle	Derived from DEM
2.	Slope Aspect	Derived from DEM
3.	Curvature	Derived from DEM
4.	Geology	DMG
5.	Soil	SOTER
6.	Distance to Stream	Derived from DEM
7.	Distance to Road	OpenStreetMap
8.	Elevation	SRTM DEM (USGS)
9.	Topographic Wetness Index	Derived from DEM
10.	Stream Power Index	Derived from DEM
11.	Rainfall	DHM
12.	Land use/ land cover	ICIMOD

2.3 Landslide Inventory Map

Landslide inventory maps are essential components of landslide susceptibility mapping providing valuable data on the location, extent, and characteristics of past landslide events within a particular area. These maps document the occurrence of landslides over time and serve as foundational datasets for assessing landslide susceptibility and risk.

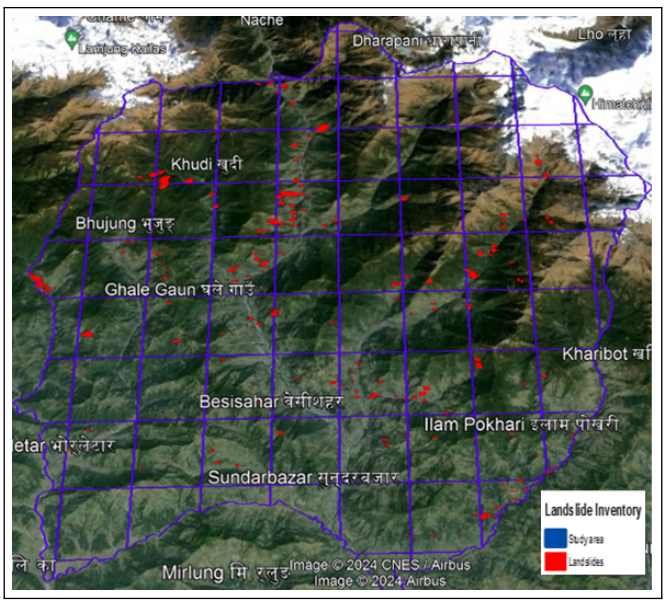

Figure 2: Landslide inventory map

For this research, the observations and digitization of landslide areas were done through visual interpretations of existing landslides on high-resolution satellite imagery, using Google Earth images. Polygons were created to map past landslides in Google Earth and processed in the GIS environment. 345 landslides were mapped in the study area covering an area of about 1.50 km^2.

2.4 Methodology

The landslide-triggering factors were developed using ArcGIS. Random points were created inside the landslide polygons to extract attributes of the landslide points in every landslide triggering factor. Similarly, the attributes of the non-landslide points were also extracted for every factor. The extracted attributes generated in the form of an Excel file were then processed in Python. The landslide and non-landslide points were divided into two datasets training (70%) and testing (30%) data set. Extremely Gradient Boosting (XGBoost) was used as the machine learning algorithm for mapping the landslide susceptibility. The model was evaluated using Accuracy, Precision, Recall, F1-Score, and Area under the ROC curve.

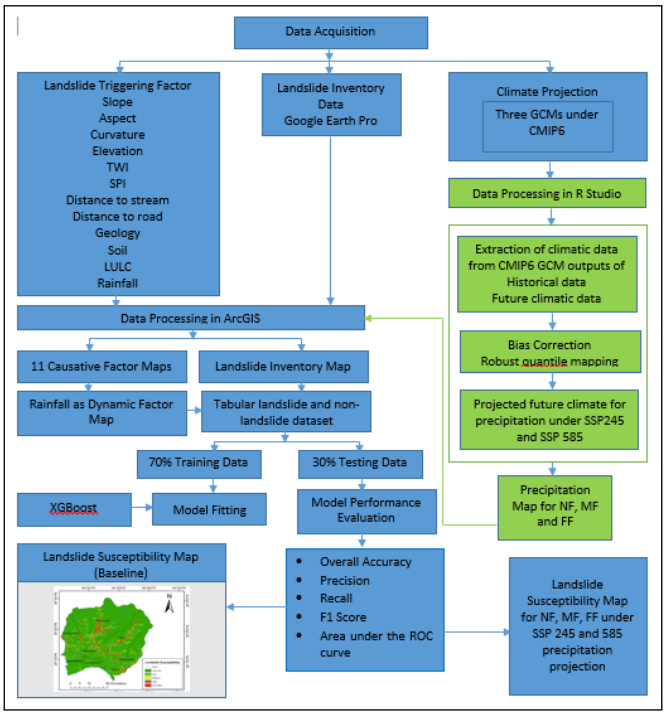

Figure 3: Methodological framework for landslide susceptibility prediction under future climate scenarios

For the future precipitation projection, the data from three GCM (Access-CM2, EC-Earth3, MPI-ESM1-2HR) under CMIP6 were downloaded and processed in R Studio. The GCMs under SSP245 and SSP585 were used to project future precipitation. The GCM projections were bias-corrected with robust empirical quantiles (RQUANT) method using the observed data from the study area to fit the GCM's coarser resolution. The projected precipitation was used to generate the future precipitation maps for three future time-frames: 2021-2045 for the near future (NF), 2046-2070 for the mid-future (MF), and 2071-2095 for the far future (FF). The precipitation maps were used as the dynamic factors to produce the future landslide susceptibility maps.

2.4.1 Extreme Gradient Boosting

XGBoost is a tree-based machine learning algorithm rooted in the gradient boosting principle that employs parallel tree boosting, allowing it to sequentially learn from the errors of previous trees. By employing gradient descent, it minimizes the loss function and mitigates overfitting. Ultimately, the predictions from all the trees are aggregated to generate the final output [20]. XGBoost uses classification and regression trees (CART) as a base learner as follows:

$$O = \sum_{i=0}^{n} L(y_i, (\hat{y}_i)) + \sum_{k=0}^{K} R(f_k) + C \quad (1)$$

Where $L(y_i, \hat{y}_i)$ is the loss function that measures the difference between the actual value y_i and predicted value $\hat{y}_i$. $R(f_k)$ is a regularization function to prevent over-fitting. K represents the number of trees (weak learners) in the ensemble.

3. Results

3.1 Model Performance

The performance of the XGBoost classification algorithm is presented in Table 2. The Accuracy and Precision values of the XGBoost model are found to be 93.8%, and 95.4% respectively. To identify the positive samples from the data, XGBoost also has a good recall value of 92.6%. The 98.2% AUC value indicates that for landslide susceptibility mapping, XGBoost is a good classifier for the study area.

Table 2: Model performance per various measures

S.N	Performance Metrics	Value
1	Accuracy	93.8%
2	Precision	95.4%
3	Recall	92.6%
4	F1-Score	93.7%
5	AUC	98.1%

The area under the ROC curve (AUC) with actual label prediction plotted in Figure 5 also indicates that XGBoost is a good classifier for landslide susceptibility mapping for the study area.

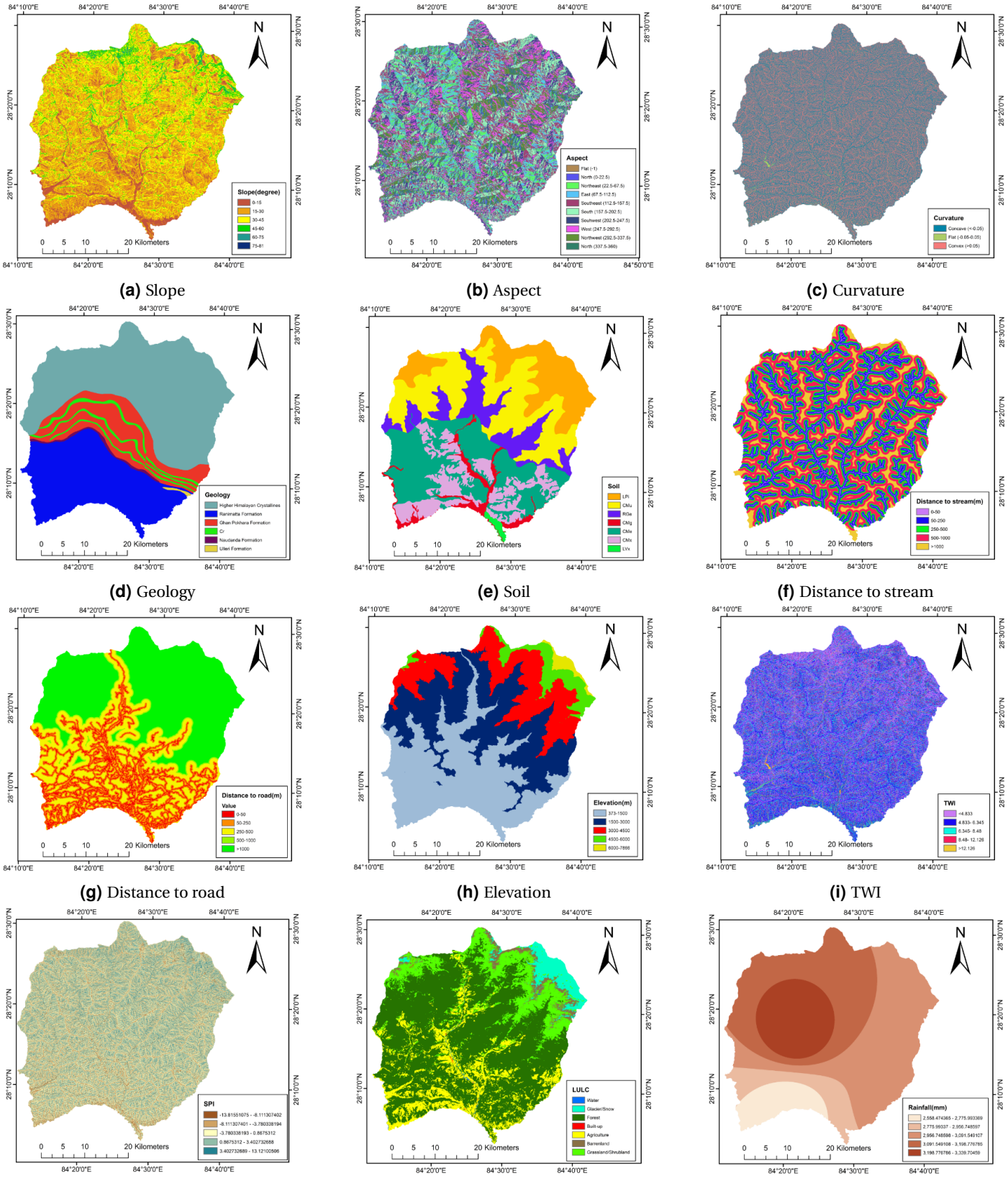

(a) Slope **(b)** Aspect **(c)** Curvature

(d) Geology **(e)** Soil **(f)** Distance to stream

(g) Distance to road **(h)** Elevation **(i)** TWI

(j) SPI **(k)** LULC **(l)** Rainfall

Figure 4: Landslide triggering factors

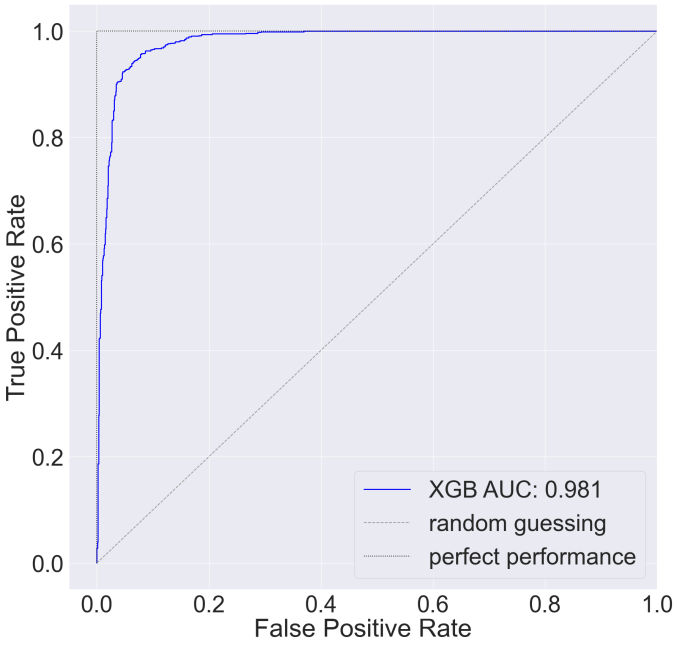

Figure 5: Area under the ROC curve

3.2 Baseline Landslide Susceptibility Map

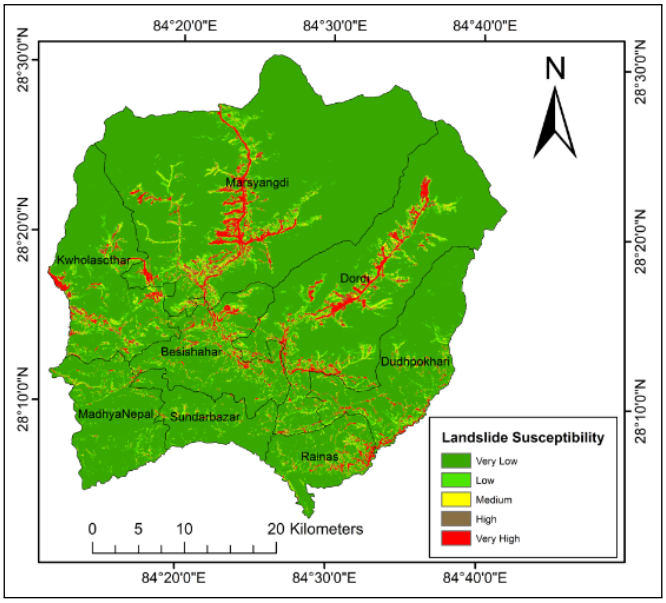

Figure 6: LSM under baseline condition

The baseline susceptibility map for the study area developed using the XGBoost algorithm is shown in Figure 6. Each susceptibility class area was calculated. Results show that 54.768 km^2 (3.29%) of the total area lies in the very high susceptibility class. Most of the study area lies within the very low susceptibility class 82.45% followed by low, moderate, and high classes with 7.08%, 3.84%, and 2.88% areas respectively (Table 3).

3.3 Municipality-wise Susceptibility Analysis

While a significant portion of the study area is categorized as having very low susceptibility, the municipality-level analysis aims to identify areas falling within the high and very high susceptibility categories. As observed in Figure 7, Dordi and Marsyangdi rural municipalities exhibit the highest susceptibility to landslides in terms of area coverage within the high and very high susceptibility classes, followed by Besishahar municipality and Kwhlosothar rural municipality, and subsequently by Dudipokhari rural municipality and Rainas municipality respectively. Conversely, Madhyanepal and Sundarbazar municipality demonstrate the lowest susceptibility to landslides respectively.

Table 3: Landslide affected area for different susceptibility classes

S.N	Susceptibility Class	Area (km^2)	Area (%)
1	Very Low	1373.66	82.45
2	Low	118.02	7.08
3	Moderate	63.95	3.84
4	High	48.04	2.88
5	Very High	54.76	3.29

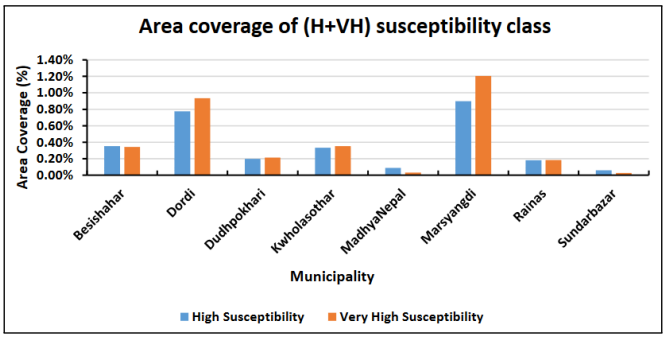

Figure 7: Area coverage percentage of high and very high (H+VH) landslide susceptibility classes within municipality

3.4 Road Exposure Assessment

The length of the road section exposed to landslides is determined by conducting spatial overlay analysis, where existing road network data is overlaid with landslide susceptibility maps within the GIS environment. The assessment of the physical exposure of the road network involves determining the ratio or proportion of road section length that could potentially be affected by landslides to the total length of the road [16]. As shown in Table 4, the majority of the road in the study area falls in the very low, at 48.56% susceptibility class, while 12.96% and 9.54% length of the road falls in the low and medium susceptibility class, respectively. Similarly, 9.99% length of the road falls in the high susceptibility class whereas 18.95% falls in the very high susceptibility class.

Table 4: Road exposure to landslide susceptibility

Landslide Susceptibility	Road Exposure Length (km)	Road Exposure Length (%)
Very Low	940.21	48.56
Low	250.96	12.96
Medium	184.63	9.54
High	193.47	9.99
Very High	366.95	18.95

3.5 Future Climate Projection

The three GCM (Access-CM2, EC-Earth3, MPI-ESM1-2HR) values were projected, and the extracted value of the relevant station was calculated. Three future time-frames were considered: 2021-2045 for the near future (NF), 2046-2070 for the mid-future (MF), and 2071-2095 for the far future (FF). The projected future values of selected GCMs were ensembled into a single value for the selected meteorological station and the annual average value was taken for the corresponding futures.

3.5.1 Precipitation Projection under SSP245 Scenario

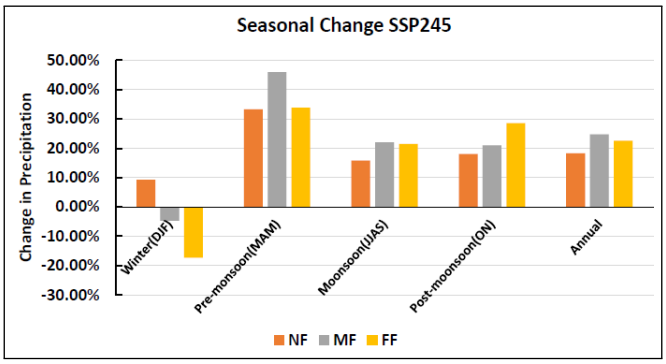

Figure 8: Seasonal precipitation projection under SSP245 scenario

Under SSP245, the average annual precipitation for the whole study region is projected to increase by 18.24% in NF, 24.76% in MF, and 22.54% in FF. On a seasonal scale, the precipitation in monsoon is projected to increase by 15.80%, 21.98%, and 21.51% for NF, MF, and FF respectively. Similarly, change in post-monsoon is projected to be 18.08%, 20.96%, and 28.54%, change in pre-monsoon is projected to be 33.26%, 45.93%, and 33.86%, change in winter precipitation is projected to be 9.26%, -4.67%, and -17.35% for NF, MF, and FF respectively.

3.5.2 Precipitation Projection under SSP585 Scenario

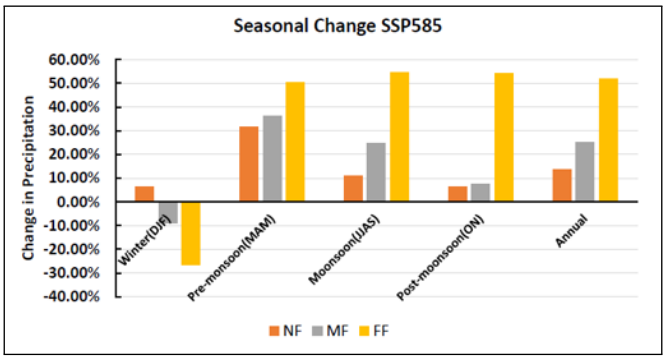

Figure 9: Seasonal precipitation projection under SSP585 scenario

Under SSP585, the average annual precipitation for the whole study region is projected to increase by 13.78% in NF, 25.07% in MF, and 51.85% in FF. On a seasonal scale, the precipitation in monsoon is projected to increase by 11.07%, 21.76%, and 54.48% for NF, MF, and FF respectively. Similarly, change in post-monsoon is projected to be 6.51%, 7.40%, and 54.20%, change in pre-monsoon is projected to be 31.58%, 36.25%, and 50.22%, change in winter precipitation is projected to be 6.32%, -8.77%, and -26.41% for NF, MF, and FF respectively.

3.6 Landslide Susceptibility Maps under Future Climate Scenarios

Six landslide susceptibility maps were generated under SSP245 and SSP585 scenarios for the near future (2021-2045), mid-future (2046-2075), and far future (2076-2095). The landslide susceptibility maps were classified into five susceptible classes in ArcGIS viz. very low, low, moderate, high, and very high (Figure 12). Area geometry was calculated to quantify the total area of landslide susceptibility.

3.6.1 Landslide Susceptibility under SSP245 Scenario

For the SSP245 scenario, in the near future, 3.56% and 2.91 % of the study area lie in the high and very high susceptibility respectively. For the mid-future, 3.26% and 3.52% of the study area lie in the high and very high susceptibility class respectively. Finally, for the far future, 3.23% and 3.40% of the study area lies in the high and very high susceptibility classes, respectively. Based on the SSP245 scenario for the near future, mid-future, and far future, the high and very high susceptibility level zones occupied approximately 6.47%, 6.78%, and 6.63% of the study area, respectively.

Table 5: Landslide susceptible area under SSP245

Susceptibility Class	SSP 245 Area(%)		
	NF	MF	FF
Very Low	81.92	80.02	80.65
Low	7.22	8.12	7.95
Moderate	3.94	4.59	4.32
High	2.91	3.26	3.23
Very High	3.56	3.52	3.40

Municipality-wise variation in the combined high and very high susceptible area (Figure 10) shows an increase for all time horizons in Besishahar, Dudhpokhari, and Madhyanepal when compared to the baseline. In Besishahar and Madhyanepal, the most significant increase in the susceptible area is observed in the mid-future period. In Dudhpokhari, the highest increase in susceptible areas occurs in the near future period.

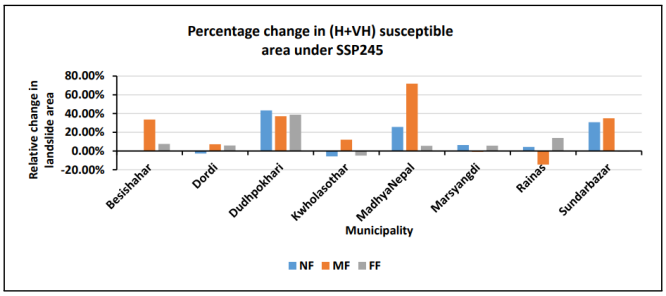

Figure 10: Relative change in combined high and very high (H+VH) susceptible area across municipalities under SSP245

In Marsyangdi and Rainas, susceptibility initially rises in the near future period, followed by a subsequent decrease in the

mid-future period, and then another increase in susceptibility in the far future period. In Sundarbazar, the susceptible area is shown to increase in the near future and mid-future periods, then decrease in the far future period. For Dordi, the susceptible area decreases in the near future period, then increases in the subsequent mid-future and far future periods. In Kwholasothar, susceptibility decreases in the near future and far future periods and increases in the mid-future period compared to the baseline.

3.6.2 Landslide Susceptibility under SSP585 Scenario

For the SSP585 scenario, in the near future, 2.92% and 3.39 % of the study area lie in the high and very high susceptibility respectively. For the mid-future, 3.47% and 3.41% of the study area lie in the high and very high susceptibility classes respectively. Finally, for the far future, 3.37% and 3.62% of the study area lies in the high and very high susceptibility classes, respectively. Based on the SSP585 scenario for near-future, mid-future, and far future, the high and very high susceptibility level zones, occupied approximately 6.31%, 6.88%, and 7.00% of the study area, respectively.

Municipality-wise variation in the combined high and very high susceptible area (Figure 12) show an increase for all time horizons in Besishahar, Dudhpokhari, Madhyanepal, Rainas, and Sundarbazar when compared to the baseline. In Besishahar and Sundarbazar, the most significant increase in the susceptible area is observed in the far future period. While in Dudhpokhari, Madhyanepal, and Rainas, the most significant increase in the susceptible area is observed in the mid-future period.

Table 6: Landslide susceptible area under SSP585

Susceptibility Class	SSP 585 Area(%)		
	NF	MF	FF
Very Low	82.17	79.86	79.98
Low	7.15	8.24	7.98
Moderate	3.92	4.57	4.58
High	2.92	3.47	3.37
Very High	3.39	3.41	3.62

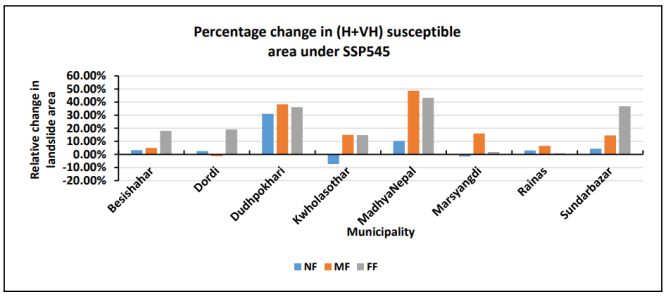

Figure 12: Relative change in combined high and very high (H+VH) susceptible area across municipalities under SSP585

In Kwholasothar and Marsyangdi, susceptibility initially decreases in the near future period, followed by a subsequent increase in the mid-future and far future period. In Dordi, the susceptible area is shown to increase in the near future and far future while decreasing in the mid-future period.

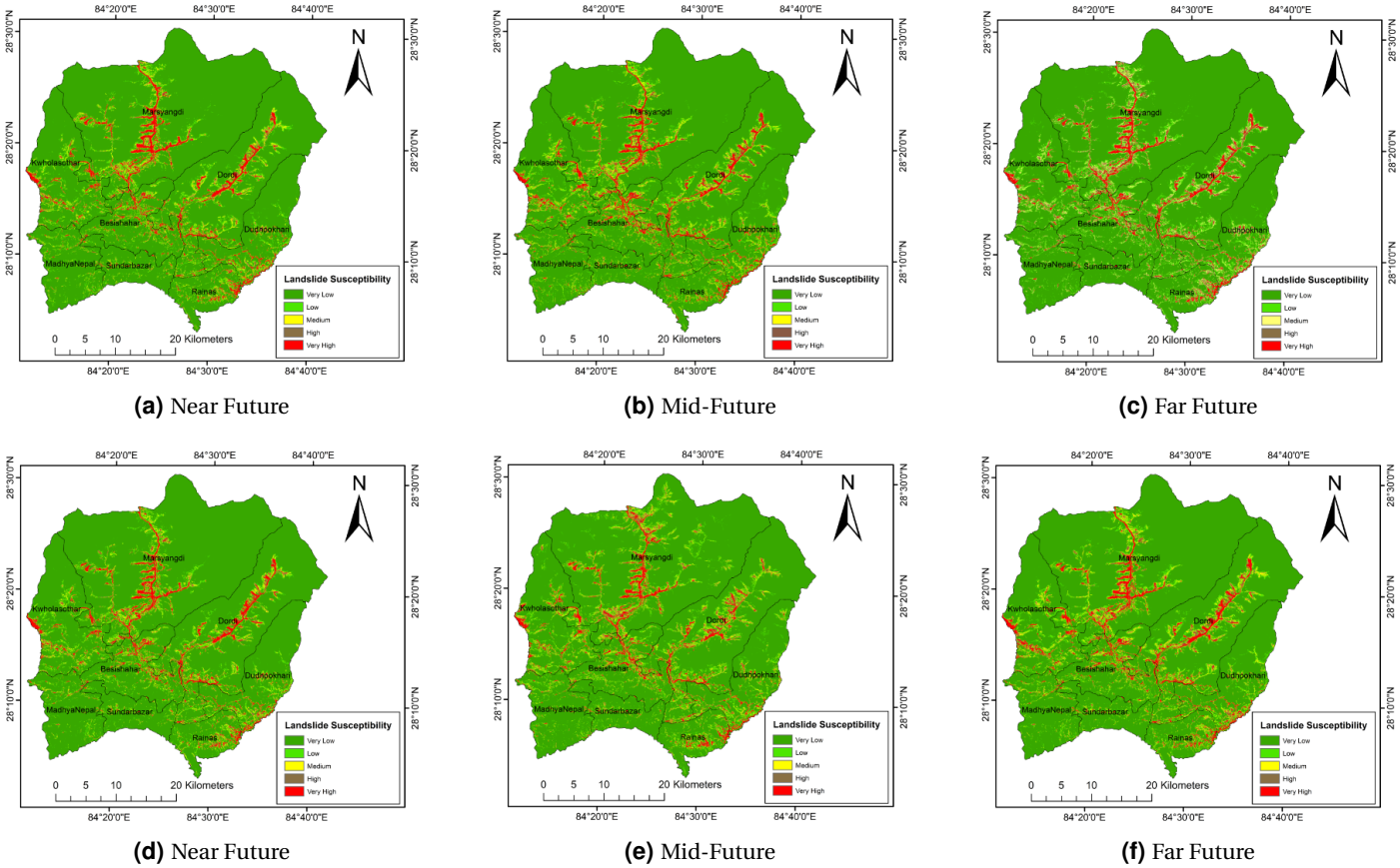

(a) Near Future **(b)** Mid-Future **(c)** Far Future

(d) Near Future **(e)** Mid-Future **(f)** Far Future

Figure 11: Landslide susceptibility map: (a),(b),(c) under SSP 245 scenario; (d),(e),(f) under SSP 585 scenario

4. Discussion

The landslide-susceptible areas are projected to increase for the future climate scenarios for both SSP245 and SSP585, in comparison to the landslide-susceptible areas modeled for the existing baseline climate conditions (1995–2020). SSP585 showed larger susceptible areas than SSP245 in all future scenarios except for the near future scenario where it shows a decrease in the susceptible areas. The susceptibility map for the SSP585 far future scenario shows the highest susceptibility compared to all other scenarios. Based on the results, it shows that under climate change scenarios exposure to landslides would increase for the study area. A similar study [16] conducted in Bagmati and Madhesh province of Nepal also found that there will be an increase in high and very high susceptible areas compared to the baseline period under future RCP4.5 and RCP8.5 climate scenarios. Landslide susceptibility maps can help land use planners with better decision-making.

In terms of area coverage within the high and very high susceptibility classes, Dordi and Marsyangdi rural municipalities show the highest susceptibility to landslides among the eight municipalities. Future landslide susceptibility scenarios show a significant increase in susceptible areas in Dudhpokhari, Kwaholasothar, Madhyanepal, and Sundarbazar. The feature importance visualization (Figure 13) shows that distance from the road and distance from the stream play a significant role in landslide susceptibility, with the spatial distribution of landslide susceptibility higher along Marsyangdi, Dordi, and Chepe River. A study conducted by Pokhrel and Pathak [21] on landslide susceptibility mapping in the southern part of the Marsyangdi River also found that higher susceptibility classes generally follow the river or road section. Assessment of road exposure to landslide susceptibility shows that 560.13 km (28.94%) of 1936.240 km road falls in the high and very high susceptibility class.

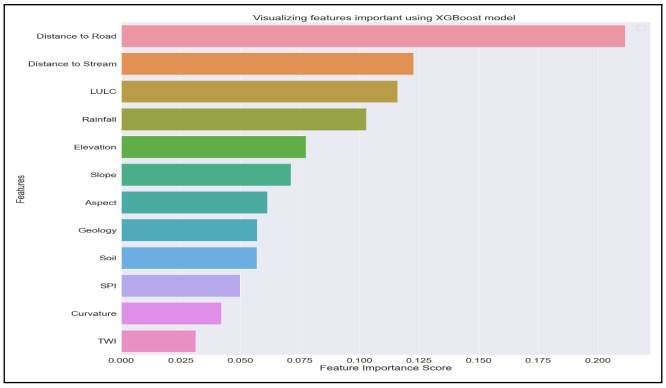

Figure 13: Feature importance

Landslide susceptibility mapping is crucial in comprehending and mitigating landslide risks in susceptible regions. They enable the identification of landslide-prone areas, empowering authorities and stakeholders to allocate resources strategically and enact suitable measures to reduce risks and enhance disaster preparedness. By integrating climate projections into susceptibility mapping models, researchers can assess how changing climatic conditions may impact landslide susceptibility in different regions. This information can help identify areas likely to experience increased landslide risk in the future, allowing for early interventions and targeted mitigation measures. Additionally, future susceptibility mapping can ensure that communities are better equipped to cope with the evolving challenges brought on by climate change.

5. Conclusion

In this study, landslide susceptibility modeling and mapping were done utilizing the XGBoost algorithm to spatially locate the regions susceptible to landslides under the current and projected future scenarios. The model was evaluated through various metrics, such as Accuracy (93.8%), Precision (95.4%), Recall (92.6%), F1-Score (93.7%), and AUC (98.1%), with the results indicating the good performance of the algorithm. Seven landslide susceptibility maps were developed representing scenarios for SSP245 and SSP585 for the near future (2021-2045), mid-future (2046-2070) and far future(2071-0295), and the current (1990-2020) baseline period. The results show an increase in the high and very high landslide susceptible areas for both SSP scenarios against the baseline period, with SSP585 far future scenario showing the largest area of susceptibility. The increase in susceptible areas indicates that an increase in rainfall due to climate change will contribute to an increase in landslides in the future. While this study only used rainfall as a dynamic factor, further research can be done by utilizing both LULC and rainfall as dynamic factors for the generation of landslide susceptibility maps under future climate scenarios.

Acknowledgments

The authors are grateful to Institute of Engineering [IOE], Pulchowk Campus, Department of Hydrology and Meteorology, Department of Mines and Geology for the coordination and guidance for data collection without which this paper would have been incomplete.

References

[1] Ranjan Kumar Dahal, Shuichi Hasegawa, Minoru Yamanaka, and K Nishino. Rainfall triggered flow-like landslides: understanding from southern hills of kathmandu, nepal and northern shikoku, japan. *Proc 10th Int Congr of IAEG, The Geological Society of London, IAEG2006 Paper*, pages 1–14, 2006.

[2] Fausto Guzzetti, Alessandro Cesare Mondini, Mauro Cardinali, Federica Fiorucci, Michele Santangelo, and Kang-Tsung Chang. Landslide inventory maps: New tools for an old problem. *Earth-Science Reviews*, 112(1-2):42–66, 2012.

[3] Khamarrul Azahari Razak, Michele Santangelo, Cees J Van Westen, Menno W Straatsma, and Steven M de Jong. Generating an optimal dtm from airborne laser scanning data for landslide mapping in a tropical forest environment. *Geomorphology*, 190:112–125, 2013.

[4] Işık Yilmaz. Landslide susceptibility mapping using frequency ratio, logistic regression, artificial neural networks and their comparison: a case study from kat

landslides (tokat—turkey). *Computers & Geosciences*, 35(6):1125–1138, 2009.

[5] Ranjan Kumar Dahal, Shuichi Hasegawa, Atsuko Nonomura, Minoru Yamanaka, Takuro Masuda, and Katsuhiro Nishino. Gis-based weights-of-evidence modelling of rainfall-induced landslides in small catchments for landslide susceptibility mapping. *Environmental Geology*, 54:311–324, 2008.

[6] Lee Moung-Jin, Song Won-Kyong, Won Joong-Sun, Park Inhye, and Lee Saro. Spatial and temporal change in landslide hazard by future climate change scenarios using probabilistic-based frequency ratio model. *Geocarto International*, 29(6):639–662, 2014.

[7] Recep Can, Sultan Kocaman, and Candan Gokceoglu. A comprehensive assessment of xgboost algorithm for landslide susceptibility mapping in the upper basin of ataturk dam, turkey. *Applied Sciences*, 11(11):4993, 2021.

[8] Ajaya Pyakurel, Bhim Kumar Dahal, and Dipendra Gautam. Does machine learning adequately predict earthquake induced landslides? *Soil Dynamics and Earthquake Engineering*, 171:107994, 2023.

[9] Abdelaziz Merghadi, Ali P Yunus, Jie Dou, Jim Whiteley, Binh ThaiPham, Dieu Tien Bui, Ram Avtar, and Boumezbeur Abderrahmane. Machine learning methods for landslide susceptibility studies: A comparative overview of algorithm performance. *Earth-Science Reviews*, 207:103225, 2020.

[10] Saraju K Baidya, Madan Lal Shrestha, and Muhammad Munir Sheikh. Trends in daily climatic extremes of temperature and precipitation in nepal. *Journal of Hydrology and Meteorology*, 5(1):38–51, 2008.

[11] Sonia Seneviratne, Neville Nicholls, David Easterling, Clare Goodess, Shinjiro Kanae, James Kossin, Yali Luo, Jose Marengo, Kathleen McInnes, Mohammad Rahimi, et al. Changes in climate extremes and their impacts on the natural physical environment. 2012.

[12] Chyi-Tyi Lee et al. Landslide trends under extreme climate events. *Terr. Atmos. Ocean. Sci*, 28(1):33–42, 2017.

[13] Huaxiang Yin, Jiahui Zhang, Sanjit Kumar Mondal, Bingwei Wang, Lingfeng Zhou, Leibin Wang, and Qigen Lin. Projected rainfall triggered landslide susceptibility changes in the hengduan mountain region, southwest china under 1.5–4.0° c warming scenarios based on cmip6 models. *Atmosphere*, 14(2):214, 2023.

[14] Constantinos Nefros, Dimitrios S Tsagkas, Gianna Kitsara, Constantinos Loupasakis, and Christos Giannakopoulos. Landslide susceptibility mapping under the climate change impact in the chania regional unit, west crete, greece. *Land*, 12(1):154, 2023.

[15] Guido Rianna, Alfredo Reder, Paola Mercogliano, and Luca Pagano. Evaluation of variations in frequency of landslide events affecting pyroclastic covers in campania region under the effect of climate changes. *Hydrology*, 4(3):34, 2017.

[16] I Putu Krishna Wijaya, Peeranan Towashiraporn, Anish Joshi, Susantha Jayasinghe, Anggraini Dewi, and Md Nurul Alam. Climate change-induced regional landslide hazard and exposure assessment for aiding climate resilient road infrastructure planning: a case study in bagmati and madhesh provinces, nepal. In *Progress in Landslide Research and Technology, Volume 1 Issue 1, 2022*, pages 175–184. Springer, 2023.

[17] David N Petley, Gareth J Hearn, Andrew Hart, Nicholas J Rosser, Stuart A Dunning, Katie Oven, and Wishart A Mitchell. Trends in landslide occurrence in nepal. *Natural hazards*, 43:23–44, 2007.

[18] Ramchandra Karki, Shabeh ul Hasson, Udo Schickhoff, Thomas Scholten, and Jürgen Böhner. Rising precipitation extremes across nepal. *Climate*, 5(1):4, 2017.

[19] Rajan KC, Keshab Sharma, Bhim Kumar Dahal, Milan Aryal, and Mandip Subedi. Study of the spatial distribution and the temporal trend of landslide disasters that occurred in the nepal himalayas from 2011 to 2020. *Environmental Earth Sciences*, 83(1):42, 2024.

[20] Jason Brownlee. *XGBoost With python: Gradient boosted trees with XGBoost and scikit-learn*. Machine Learning Mastery, 2016.

[21] Prakash Pokhrel and Dinesh Pathak. Landslide susceptibility mapping of southern part of marsyangdi river basin, west nepal using logistic regression method. *International Journal of Geomatics and Geosciences*, 7(1):24–32, 2016.